A Coordinated Two-stage Decentralized Flexibility Trading in Distribution Grids with MGs

Tao Xu, Rujing Wang, He Meng,Mengchao Li, Hongru Wang, Yu Ji, Ying Zhang, Qingrong Zheng, Ping Song, and Jiani Xiang

***Abstract*—Renewable energy dominated future power grids require enhanced system flexibility, in particular, activating the participation from various distributed energy resources (DERs). A coordinated two-stage flexibility trading framework for distribution system with microgrids (MGs) is proposed in this paper. At day-ahead stage, a peer to peer (P2P) trading mechanism and the associate leasing strategy of shared energy storage system are performed to solve the power variations caused by the wide spread integration of renewable resources, where asymmetric Nash bargaining is used to realize the fair revenue allocation according to the contribution of each MG in P2P trading. At intra-day stage, given the power imbalances from unexpected uncertainties, MGs exploit the adjustability of the DERs in responding to rapid flexibility requirements issued by distribution system operator. In particular, the average consensus based decentralized Newton method with super linear convergence is utilized to meet the requirements of flexibility while maintaining the information security. The feasibility, effectiveness and equity of the proposed trading strategies are verified through various simulation studies.**

***Index Terms*—Microgrids, decentralized Newton, flexibility trading, asymmetric Nash bargaining, peer-to-peer.**

I. Introduction

In order to mitigate the energy crisis and greenhouse gas (GHG) emission effect caused by the excessive consumption of fossil fuels for the past decades, consensus has been incentivized worldwide on developing renewable energy (RE) in a sustainable approach. Global activities have been made in accelerating the energy transitions in recent years. In 2019, the U.K. government released the 'Energy White Paper' to specify the goal towards net zero by 2050 [1]. At the same year, the 'European Green Deal' has been issued to ensure efficient portfolio in reaching net zero in the EU by 2050 [2]. In 2021, the U.S. government released the 'Executive Order 14008' on tackling the climate crisis to achieve a carbon pollution-free electricity before 2035 [3]. As the world's largest energy consumer and carbon emitter, China pledged the energy transition plan in 2020 with a target of achieving country-wide carbon neutrality by 2060 [4].

According to the announced pledges, the International Energy Agency has estimated that the proportion of RE generation in China is expected to reach 60% [4] while the EU and U.S. plan to reach 100% [5] and 80% [6] by 2050, respectively. The RE dominated electric power grid, and in particular the distribution system, poses significant challenges to the system's operation and control [7]. To address the challenges, instead of network infrastructure reinforcement, sufficient and active system regulation capabilities, namely system flexibility, in multiple time scales is urgently required [8].

The concept of grid flexibility is still emerging, and can be illustrated as the flexible margin to accommodate REs [9], or the system efficiency in responding changing scenarios [10]. At power distribution grids, operators aim to maintain a diversified portfolio of flexible schemes at various time scales without additional investment, making full utilizations of distributed energy resources (DERs) including controllable distributed generation (DG), energy storage systems (ESSs), flexible loads, or in an integrated form as microgrids (MGs). In this paper, the grid flexibility is defined as the capability to cope with the system fluctuations at various time scales with multiple flexible resources (FRs) while pursuing cost minimization.

Received: November 18, 2023
Accepted: April 23, 2024
Published Online: September 1, 2024

Tao Xu (corresponding author), Rujing Wang, He Meng, Mengchao Li, and Hongru Wang are with the Key Laboratory of Smart Grid of Ministry of Education, Tianjin University, Tianjin 300072, China (e-mail: taoxu2011@tju.edu.cn; wrj2021@ tju.edu.cn; he_meng 2017@tju.edu.cn; lmc2021@tju.edu.cn; 3018001399@tju.edu.cn).

Yu Ji and Ying Zhang are with the State Grid Shanghai Energy Interconnection Research Institute Co., Ltd., Shanghai 200031, China (e-mail: jiyu@epri.sgcc.com.cn; zhangying@epri.sgcc.com.cn).

Qingrong Zheng is with the Key Laboratory of Smart Grid Demand Response, Shanghai 200030, China (e-mail:zhengqr@sh. sgcc.com.cn).

Ping Song and Jiani Xiang are with the State Grid Shanghai Municipal Electric Power Company, Shanghai 200122, China (e-mail: songp@sh.sgcc.com.cn; 934714165@qq.com).

DOI: 10.23919/PCMP.2023.000178

The flexibility market has attracted substantial attentions globally. There are two major trends on market mechanisms. One aspect is the design of commercial products to bring rapid flexibility services to the grid [11], [12]. The U.K. National Grid developed optional downward flexibility management [11], whereas the flexible ramping product introduced by the independent system operator (ISO) in the U.S., can reach MW-level output within 10 minutes [12]. It can be seen that the current flexibility products are mainly on transmission level with certain entry thresholds.

The other aspect is the local flexibility markets that provide options for flexibility trading among participants in active distribution networks (ADNs) [13]. The introduction of flexibility services on ADNs can incentivize broader participation through flexibility bidding [14], flexibility tokens [15], and flexibility contracts [16], etc. Meanwhile, the efficient integration and utilization of FRs can achieve better system performances, i.e., preventing overloading issues [17] and relieving system congestion [18]. Therefore, the local flexibility market not only maximizes the flexibility potential and lowers the access threshold for DER participation, but also relieves the regulation pressure of the higher voltage grid. However, the proposed local flexibility markets mechanisms need to be further developed to better cope with the actual energy market framework, in particular, the coordination and aggregation among resources with different source-load characteristics need to be further explored to enhance the overall system operational flexibility and economy.

Among different types of participants in local flexibility markets, MG is one of the integrated approaches for DERs. MGs with different source-load characteristics can promote consumption of REs and achieve win-win benefits through information exchange and peer-to-peer (P2P) trading [19], coordination among multi-microgrids (MMGs) can also be considered as an extension of flexibility trading [20].

Existing research on P2P trading can be divided into three categories: centralized, decentralized, and distributed. In centralized approach, a coordinator who communicates with all participants is used to make decisions on transaction prices and to allocate revenues based on pre-determined rules [21], [22]. In [21], the coordinator can assign fixed prices for P2P transactions between houses that are equipped with roof photovoltaic (PV) and battery packs. Reference [22] proposes a centralized P2P transactions scheme named smart electricity exchange platform (STEP), where the trading prices are specified in advance as a constraint.

In decentralized trading, the information privacy of participants is well protected without third-party involvement. There are various forms of approaches, including bilateral contract networks, consensus approaches, blockchain mechanisms and multi-agent systems. In [23], a decentralized P2P energy trading strategy is proposed in blockchain environment based on consensus algorithm. The scheme proposed in [24] respects market players' preferences by allowing bilateral energy trading with product differentiation.

Combined with centralized and decentralized approaches, the distributed trading operates in a decentralized manner although the communication among prosumers is in a centralized fashion [25], [26]. Coordinators tend to indirectly influence users through appropriate price signals. In [25], the P2P-based flexibility service is implemented between MGs under the system-level regulation of distribution system operator (DSO), where the chance-constrained uncertainty distribution locational marginal price (CC-UDLMP) is used to settle the transactions. Reference [26] proposes a P2P energy trading mechanism based on divided transaction zones, to guide the trading of prosumers in the same zone to avoid the network congestions. Despite the fact that energy sharing among participants has been investigated in a variety of practices, few have discovered the potential of DERs to support flexibility on the distribution grid.

In order to identify the gaps between existing research and this study, a comparison on the existing research related to the flexibility markets is shown in Table I.

TABLE I
A SUMMARY AND COMPARISON AMONG EXISTING LITERATURE ON FLEXIBILITY TRADING

Ref.	System flexibility	Local flexibility market	P2P	Decentralized optimization methods	Pricing based on game theory	SESS	MG
[9], [10]	√	×	×	×	×	×	×
[11]	√	×	×	×	×	×	×
[12]	√	×	×	×	×	×	×
[14]	√	√	×	×	×	×	×
[15]	√	√	√	√	×	×	×
[16]	√	√	×	√	×	×	×
[17], [18]	√	√	×	×	×	×	×
[19]	×	×	√	√	√	×	√
[20]	×	×	×	√	×	×	√
[21], [22]	×	×	√	×	×	×	×
[23]	×	×	√	√	√	×	×
[24]	×	×	√	√	×	×	×
[25]	√	√	√	√	√	×	√
[26]	×	×	√	×	√	×	×
This paper	√	√	√	√	√	√	√

The literature has discussed various motivations and strategies to encourage participants to actively involve the local flexibility market. However, the following aspects need further investigation to ensure practical implementation: 1) the power fluctuations in light of volatile REs need to be resolved hieratically to better compensate the unexpected uncertainties; 2) the vitality and responsivity of FRs need to be further stimulated in the context of information security; 3) the fair allocation strategies among participants need to be practical and executable; and 4) the high efficiency computation is required to ensure rapid responses and practical implementations for local flexibility services.

Therefore, the main purpose of this paper is to propose a practical two-stage flexibility trading framework among MGs to enhance the system flexibility. At day-ahead stage, a P2P trading mechanism of MMGs and associate leasing strategy of a shared energy storage system (SESS) are introduced to solve the power variations caused by the integration of REs. At intra-day stage, considering the short-term power fluctuations that are not solved at day-ahead stage, a fully decentralized optimization algorithm is developed to address the rapid response requirements on flexibility. The case studies verify the feasibility of the proposed methodology and algorithm. The main contributions of this paper can thus be summarized as follows:

1) A coordinated two-stage decentralized trading framework is established to enhance the system flexibility by coping with the medium-term power variations at day-ahead stage, and short-term power unbalance at intra-day stage.

2) A decentralized alternating direction method of multipliers (ADMM) and a decentralized Newton algorithm are developed with the consideration of the information security.

3) An asymmetric Nash bargaining method is proposed to realize the fair revenue allocation according to the contribution of each MG in P2P trading process.

4) An average consensus based decentralized Newton method combining privacy protection and computing performance is proposed to solve the flexible resource allocation effectively among MGs at intra-day stage.

II. Framework of the Coordinated Two-stage Flexibility Trading

A. Overview of the Framework

As shown in Fig. 1, M MGs ($\mathcal{M}=\{1,\cdots,M\}$) are integrated to the distribution grid, where energy and information are exchanged with each other through a common busbar and a communication network. Each MG_i ($i\in\mathcal{M}$) contains various types of DERs, including local RE generation, battery energy storage system (BESS), microturbine (MT) and elastic loads.

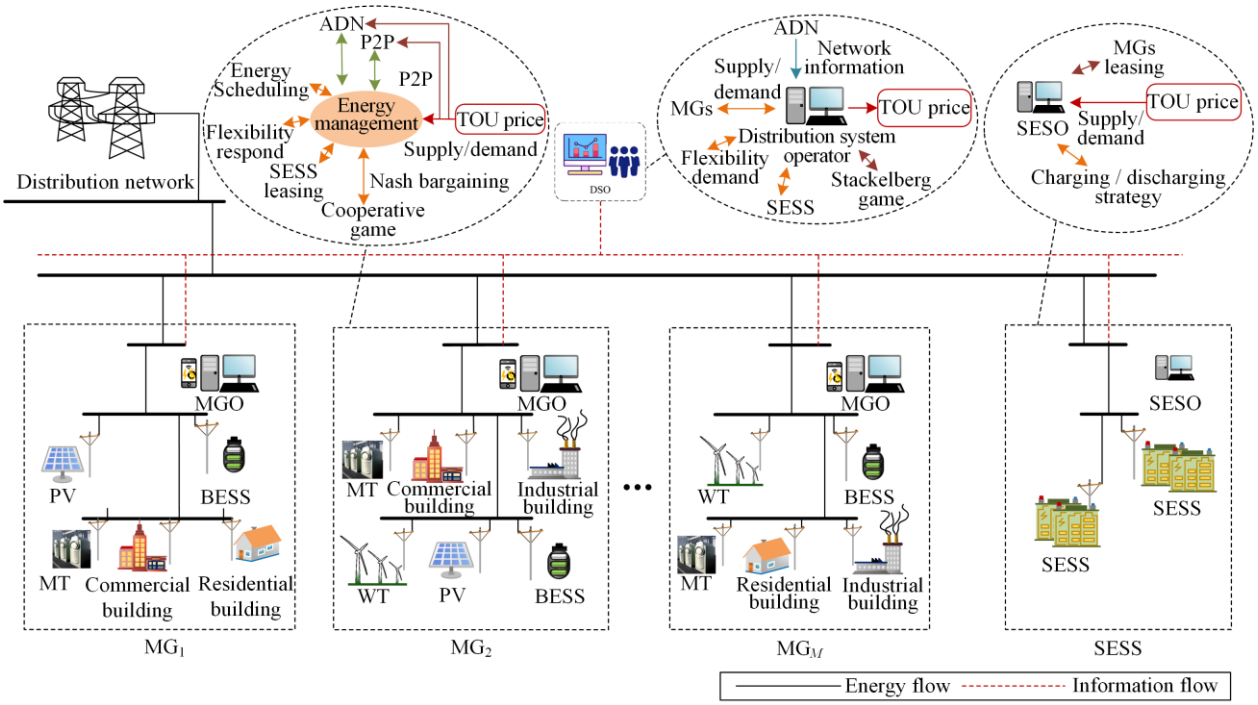

Fig. 1. Framework of the proposed two-stage flexibility trading.

Three stakeholders can be identified, namely, MG operators (MGOs), shared energy storage operator (SESO) and DSO. Basically, the MGO manages the energy trading and power scheduling by utilizing local FRs; the SESO governs the charging/discharging activities and associate leasing fees; and the DSO is responsible for the overall system operation while maintaining the system flexibility.

B. The Mechanism of Two-stage Flexibility Trading

The mechanism of the proposed flexibility trading can be divided into day-ahead stage and intra-day stage, as shown in Fig. 2(a) and Fig. 2(b), respectively.

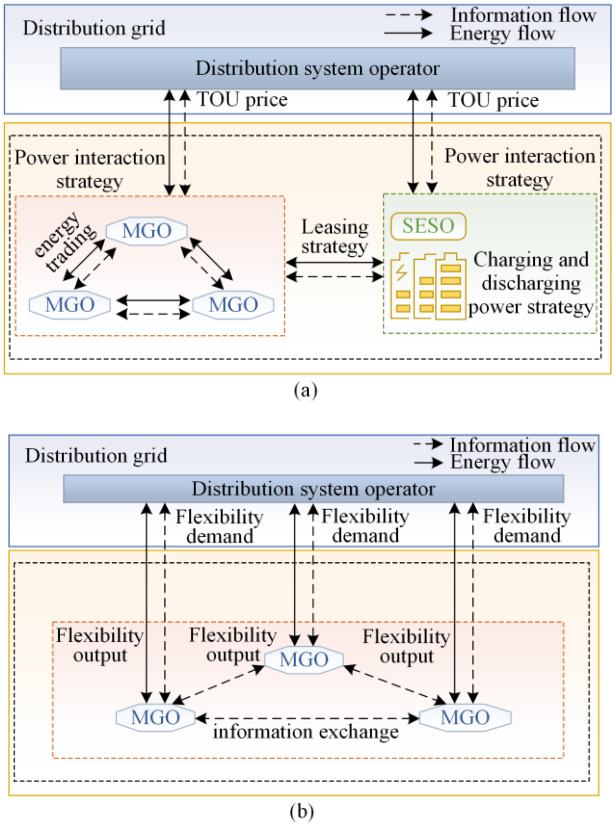

Fig. 2. The mechanism of two-stage flexibility trading. (a) The day-ahead stage flexibility trading. (b) The intra-day stage flexibility trading.

At day-ahead stage, the daily operation horizon can be divided into 24 time slots, denoted as $\mathcal{T}=\{1,\cdots,T\}$. As the leader, DSO formulates time of use (TOU) pricing according to net load profiles to encourage participation in peak-valley regulation. MGOs implement a two-layer scheduling strategy to promote the local consumption of REs. On the upper layer, each MGO develops and submits the charging and discharging requirements to SESS to smooth out the power fluctuations, while the SESO aggregates the information and determines the leasing services according to the specified tariff. On the lower layer, MGOs implement the P2P energy trading and scheduling to activate the flexibility potential of DERs, as well as the revenue allocation via decentralized strategy based on asymmetry Nash bargaining. The optimal energy trading strategy can be determined with energy trading quantity negotiation and energy trading price negotiation, sequentially.

At intra-day stage, the DSO broadcasts the flexibility demand caused by unexpected power imbalance, which can be adjusted via energy interaction between ADN and MGs at every 15 min. The MG alliance achieves optimal allocation of FRs at minimal cost through a decentralized strategy. It is worth noting that the state of charge (SOC) of SESS is already managed in an appropriate state at day-ahead stage, so SESS is ignored for flexible trading at intra-day stage.

III. Mathematical Formulation

A. Day-ahead Scheduling

1) The Optimization Model of DSO

The ADN's net load can be described as:

$$P^t_{\mathrm{ADN,net}} = P^t_{\mathrm{ADN,L}} - P^t_{\mathrm{ADN,e}} \tag{1}$$

where $P^t_{\mathrm{ADN,e}}$ and $P^t_{\mathrm{ADN,L}}$ are the total REs power output and the load of ADN, respectively.

The decision variable of DSO is TOU sale price with the optimization objective of operational revenue maximization, i.e.:

$$\max U_{\mathrm{ADN}} = I_{\mathrm{MMG}} + I_{\mathrm{SESS}} - C_{\mathrm{grid}} \tag{2}$$

where I_{MMG} and I_{SESS} are the power trading revenues of DSO with MGOs and SESO, respectively; C_{grid} is the procurement cost from the upper grid. I_{MMG} is shown as (3)–(5).

$$\begin{cases} I_{\mathrm{MMG}} = \sum_{t=1}^{T} (\rho^t_{\mathrm{s}} P^t_{\mathrm{MMG,b}} - \rho^t_{\mathrm{b}} P^t_{\mathrm{MMG,s}}) \\ P^t_{\mathrm{MMG,s}} = \sum_{i=1}^{M} P^t_{\mathrm{MG}i,\mathrm{s}} \\ P^t_{\mathrm{MMG,b}} = \sum_{i=1}^{M} P^t_{\mathrm{MG}i,\mathrm{b}} \end{cases} \tag{3}$$

where ρ^t_{s} and ρ^t_{b} are the TOU sale and purchase prices of AND; while $P^t_{\mathrm{MG}i,\mathrm{s}}$ and $P^t_{\mathrm{MG}i,\mathrm{b}}$ are the power interaction between MG$_i$ and ADN.

$$I_{\mathrm{SESS}} = \sum_{t=1}^{T} (\rho^t_{\mathrm{s}} P^t_{\mathrm{SESS,b}} - \rho^t_{\mathrm{b}} P^t_{\mathrm{SESS,s}}) \tag{4}$$

where $P^t_{\mathrm{SESS,s}}$ and $P^t_{\mathrm{SESS,b}}$ are the charging/discharging power of SESO to DSO.

$$C_{\mathrm{grid}} = \sum_{t=1}^{T} g^t_{\mathrm{s}} P^t_{\mathrm{ADN,b}} \tag{5}$$

where g^t_{s} is the electricity price of the main grid; and $P^t_{\mathrm{ADN,b}}$ is the power purchase ADN.

The operation constraints are:

$$\rho^t_{\mathrm{s}} > \rho^t_{\mathrm{b}} \tag{6}$$

$$\sum_{t=1}^{T} \rho^t_{\mathrm{s}} \leqslant T \bar{\rho}_{\mathrm{s\cdot max}} \tag{7}$$

where $\bar{\rho}_{\mathrm{s\cdot max}}$ is the upper limit of the average TOU sale price. Equation (7) is established to avoid monopoly pricing of DSO.

2) The Optimization Model of Upper Layer

For each MGO, in order to balance the effect in smoothing the power fluctuations and the leasing cost of

SESS, a multi-objective optimization model is constructed.

MG objective 1: Net load mean square deviation minimization.

$$\min f_1 = \sum_{t=1}^{T}(P_{\mathrm{MG}i,\mathrm{L}}^t - P_{\mathrm{MG}i,\mathrm{e}}^t + P_{\mathrm{MG}i,\mathrm{c}}^t - P_{\mathrm{MG}i,\mathrm{d}}^t - P_{\mathrm{MG}i,\mathrm{ave}})^2 \tag{8}$$

$$P_{\mathrm{MG}i,\mathrm{ave}} = \sum_{t=1}^{T}(P_{\mathrm{MG}i,\mathrm{L}}^t - P_{\mathrm{MG}i,\mathrm{e}}^t + P_{\mathrm{MG}i,\mathrm{c}}^t - P_{\mathrm{MG}i,\mathrm{d}}^t)/T \tag{9}$$

where $P_{\mathrm{MG}i,\mathrm{L}}^t$, $P_{\mathrm{MG}i,\mathrm{e}}^t$, $P_{\mathrm{MG}i,\mathrm{ave}}$, $P_{\mathrm{MG}i,\mathrm{c}}^t$ and $P_{\mathrm{MG}i,\mathrm{d}}^t$ represent the load, total REs generation, equivalent average load, charging and discharging power demand of MG_i to SESS, respectively.

MG objective 2: SESS leasing cost minimization.

$$\min f_2 = uE_{\mathrm{MG}i}^{\mathrm{Lea}} + vP_{\mathrm{MG}i}^{\mathrm{Lea}} + w\sum_{t=1}^{T}(P_{\mathrm{MG}i,\mathrm{c}}^t + P_{\mathrm{MG}i,\mathrm{d}}^t) \tag{10}$$

where u, v, and w are the unit energy capacity leasing cost, unit rated power leasing cost and unit power charging/ discharging cost of SESS, respectively; $P_{\mathrm{MG}i}^{\mathrm{Lea}}$ is the rated power demand for MG_i to lease SESS, i.e., $\max\left\{P_{\mathrm{MG}i,\mathrm{c}}^t, P_{\mathrm{MG}i,\mathrm{d}}^t\right\}$; $E_{\mathrm{MG}i}^{\mathrm{Lea}}$ is the power capacity demand calculated as:

$$E_{\mathrm{MG}i}^{\mathrm{Lea}} = \alpha_{\mathrm{Lea}}(E_{\mathrm{MG}i,\max}^t - E_{\mathrm{MG}i,\min}^t) \tag{11}$$

where α_{Lea} denotes the capacity margin factor; while $E_{\mathrm{MG}i,\max}^t$ and $E_{\mathrm{MG}i,\min}^t$ are the maximum and minimum energy storage capacities for MG_i to lease SESS in the dispatching cycle, respectively.

The operation constraints are:

$$\sum_{t=1}^{T}(\eta_{\mathrm{c}}P_{\mathrm{MG}i,\mathrm{c}}^t - P_{\mathrm{MG}i,\mathrm{d}}^t/\eta_{\mathrm{d}}) = 0 \tag{12}$$

where η_{c} and η_{d} are the charging and discharging efficiency of SESS. SESO aggregates power demands from MGs as $P_{\mathrm{MG}\Sigma}^t$, whereas $P_{\mathrm{MG}\Sigma}^t > 0$ indicates charging demand to SESS.

$$P_{\mathrm{MG}\Sigma}^t = \sum_{i=1}^{M}(P_{\mathrm{MG}i,\mathrm{c}}^t - P_{\mathrm{MG}i,\mathrm{d}}^t) \tag{14}$$

The objective function of SESO is to maximize the operational revenue as shown in (15).

SESO objective:

$$\max U_{\mathrm{SESS}} = I_{\mathrm{ADN}} - C_{\mathrm{SESS}} \tag{15}$$

$$I_{\mathrm{ADN}} = \sum_{t=1}^{T}(\rho_{\mathrm{b}}^t P_{\mathrm{SESS,s}}^t - \rho_{\mathrm{s}}^t P_{\mathrm{SESS,b}}^t) \tag{16}$$

$$C_{\mathrm{SESS}} = \sum_{t=1}^{T}\zeta_{\mathrm{s}}(P_{\mathrm{SESS,c}}^t + P_{\mathrm{SESS,d}}^t) \tag{17}$$

where I_{ADN} is the arbitrage revenue of SESO; C_{SESS} is the operation cost of SESS; $P_{\mathrm{SESS,c}}^t$ and $P_{\mathrm{SESS,d}}^t$ are the charging and discharging power of SESS; and ζ_{s} is the unit operation cost of SESS. The operation constraints are as follows.

1) Power constraints of SESS:

$$\begin{cases} 0 \leqslant P_{\mathrm{SESS,c}}^t \leqslant P_{\mathrm{SESS}}^{\max},\ P_{\mathrm{MG}\Sigma}^t \geqslant 0 \\ 0 \leqslant P_{\mathrm{SESS,d}}^t \leqslant P_{\mathrm{SESS}}^{\max},\ P_{\mathrm{MG}\Sigma}^t < 0 \\ P_{\mathrm{SESS,c}}^t P_{\mathrm{SESS,d}}^t = 0 \end{cases} \tag{18}$$

where $P_{\mathrm{SESS}}^{\max}$ is the maximum charging or discharging power of SESS.

2) Stored energy constraints of SESS:

$$\mu_{\mathrm{s}}E_{\mathrm{SESS}}^{\max} \leqslant E_{\mathrm{SESS}}^t \leqslant E_{\mathrm{SESS}}^{\max} \tag{19}$$

$$E_{\mathrm{SESS}}^t = E_{\mathrm{SESS}}^{t-1} + \Delta t(\eta_{\mathrm{c}}P_{\mathrm{SESS,c}}^t - P_{\mathrm{SESS,d}}^t/\eta_{\mathrm{d}}) \tag{20}$$

where μ_{s} is the proportion of spare capacity of SESS; E_{SESS}^t is the energy capacity of SESS; and $E_{\mathrm{SESS}}^{\max}$ is the maximum energy capacity of SESS.

3) Power balance constraint:

$$P_{\mathrm{MG}\Sigma}^t + \sigma_{\mathrm{s,buy}}^t P_{\mathrm{SESS,b}}^t - \sigma_{\mathrm{s,sell}}^t P_{\mathrm{SESS,s}}^t = P_{\mathrm{SESS,c}}^t - P_{\mathrm{SESS,d}}^t \tag{21}$$

where $P_{\mathrm{MG}\Sigma}^t$ is the total charging and discharging power demands from MGs; $P_{\mathrm{SESS,b}}^t$ and $P_{\mathrm{SESS,s}}^t$ are the sale and purchase power of SESS to ADN, respectively; $\sigma_{\mathrm{s,buy}}^t$ and $\sigma_{\mathrm{s,sell}}^t$ are 0–1 representing the interaction status of SESS and ADN.

3) The Optimization Model of Lower Layer

a) P2P Trading Among MGs

Each MG regenerates the equivalent power profile after smoothing the fluctuations via leasing SESS:

$$P_{\mathrm{MG}i,\mathrm{equ}} = P_{\mathrm{MG}i,\mathrm{L}}^t + P_{\mathrm{MG}i,\mathrm{c}}^t - P_{\mathrm{MG}i,\mathrm{d}}^t \tag{22}$$

The objective function of MG_i in energy trading with other MGs can be written as:

$$\min C_i^{\mathrm{C}} = C_i^{\mathrm{N}} + C_i^{\mathrm{net}} + C_i^{\mathrm{P2P}} \tag{23}$$

where C_i^{net} is the transmission fees between MG_i and MG_j; C_i^{P2P} is the payment that MG_i bargains with other MGs; C_i^{N} is the social cost of MG_i without considering the P2P trading among MGs, which is composed of the interaction revenue with ADN ($I_{i,\mathrm{ADN}}$), the operating cost of BESS ($C_{i,\mathrm{BESS}}$), the compensation cost of elastic load ($C_{i,\mathrm{L}}$), and the generation cost of MT ($C_{i,\mathrm{MT}}$).

$$\begin{cases} C_i^{\mathrm{N}} = C_{i,\mathrm{BESS}} + C_{i,\mathrm{L}} + C_{i,\mathrm{MT}} - I_{i,\mathrm{ADN}} \\ I_{i,\mathrm{ADN}} = \sum_{t=1}^{T}(\rho_{\mathrm{b}}^t P_{\mathrm{MG}i,\mathrm{s}}^t - \rho_{\mathrm{s}}^t P_{\mathrm{MG}i,\mathrm{b}}^t) \\ C_{i,\mathrm{BESS}} = \sum_{t=1}^{T}\zeta_{\mathrm{b}}(P_{i,\mathrm{Bch}}^t + P_{i,\mathrm{Bdis}}^t) \\ C_{i,\mathrm{L}} = \sum_{t=1}^{T}\lambda_{\mathrm{e}}^{\mathrm{tran}}P_{i,\mathrm{tran}}^t \\ C_{i,\mathrm{MT}} = \sum_{t=1}^{T}(a_{\mathrm{M}i}(P_{i,\mathrm{MT}}^t)^2 + b_{\mathrm{M}i}P_{i,\mathrm{MT}}^t + c_{\mathrm{M}i}) \end{cases} \tag{24}$$

where ζ_{b} denotes the unit degradation cost of BESS; $P^t_{i,\mathrm{Bch}}$ and $P^t_{i,\mathrm{Bdis}}$ are the charging and discharging power of BESS; $\lambda^{\mathrm{tran}}_{\mathrm{e}}$ is the unit compensation cost of elastic load; and $P^t_{i,\mathrm{tran}}$ is the responsive load; $a_{\mathrm{M}i}$, $b_{\mathrm{M}i}$, and $c_{\mathrm{M}i}$ are the generation cost factor of MT; while $P^t_{i,\mathrm{MT}}$ is the power output of MT.

It's worth noting that the network loss is ignored by assuming MGs are located close to each other. Transmission fees between MG$_i$ and MG$_j$ can be calculated as:

$$C^{\mathrm{net}}_i = \frac{1}{2}\sum_{t=1}^{T}\sum_{j\in\mathcal{M}/i}\gamma^{\mathrm{e}}_1(P^t_{ij})^2 + \gamma^{\mathrm{e}}_2\left|P^t_{ij}\right| \tag{25}$$

where P^t_{ij} is the power exchange between MG$_i$ and MG$_j$, $P^t_{ij} > 0$ when MG$_i$ sells energy to MG$_j$ and $P^t_{ij} < 0$ when MG$_i$ purchases energy from MG$_j$; γ^{e}_1 and γ^{e}_2 are the transmission cost factors.

The payment that MG$_i$ bargains with other MGs is:

$$C^{\mathrm{P2P}}_i = \sum_{t=1}^{T}\sum_{j\in\mathcal{M}/i}\rho^t_{ij}P^t_{ij} \tag{26}$$

where ρ^t_{ij} denotes the trading price between MG$_i$ and MG$_j$.

The operation constraints are as follows.

1) Power balance constraint:

$$P^t_{\mathrm{MG}i,\mathrm{e}} + P^t_{i,\mathrm{MT}} - P^t_{i,\mathrm{Bch}} + P^t_{i,\mathrm{Bdis}} + P^t_{\mathrm{MG}i,\mathrm{b}} - P^t_{\mathrm{MG}i,\mathrm{s}} = P^t_{\mathrm{MG}i,\mathrm{equ}} - P^t_{i,\mathrm{tran}} + \sum_{j\in\mathcal{M}/i}P^t_{ij} \tag{27}$$

2) Network congestion constraint:

$$\begin{cases} 0 \leqslant P^t_{\mathrm{MG}i,\mathrm{s}} \\ P^t_{\mathrm{MG}i,\mathrm{b}} \leqslant P^{\max}_{\mathrm{grid}} \end{cases} \tag{28}$$

where $P^{\max}_{\mathrm{grid}}$ is the upper limit for the power interaction between MG$_i$ and ADN.

3) Operation constraints of MT:

$$P^{\min}_{\mathrm{MT}} \leqslant P^t_{i,\mathrm{MT}} \leqslant P^{\max}_{\mathrm{MT}} \tag{29}$$

where $P^{\min}_{\mathrm{MT}}$ and $P^{\max}_{\mathrm{MT}}$ are the minimum and maximum power output of MT, respectively.

4) Responsive load constraint:

$$\sum_{t=1}^{T}P^t_{i,\mathrm{tran}} = 0 \tag{30}$$

$$-\alpha_{i,\mathrm{tran}}P^t_{\mathrm{MG}i,\mathrm{L}} \leqslant P^t_{i,\mathrm{tran}} \leqslant \alpha_{i,\mathrm{tran}}P^t_{\mathrm{MG}i,\mathrm{L}} \tag{31}$$

where $\alpha_{i,\mathrm{tran}}$ is the ratio of responsive load.

5) BESS constraints:

$$\begin{cases} S^t_i = S^{t-1}_i(1-\theta_i) + \Delta t(\eta_{i,\mathrm{c}}P^t_{i,\mathrm{Bch}} - P^t_{i,\mathrm{Bdis}}/\eta_{i,\mathrm{d}}) \\ 0 \leqslant P^t_{i,\mathrm{Bch}} \leqslant P^{\max}_{i,\mathrm{Bch}}, 0 \leqslant P^t_{i,\mathrm{Bdis}} \leqslant P^{\max}_{i,\mathrm{Bdis}} \\ P^t_{i,\mathrm{Bch}}P^t_{i,\mathrm{Bdis}} = 0 \\ S^{\min}_i \leqslant S^t_i \leqslant S^{\max}_i \\ S^0_i = S^T_i \end{cases} \tag{32}$$

where S^t_i is the energy capacity of BESS; θ_i is the self-loss factor of BESS; while $\eta_{i,\mathrm{c}}$ and $\eta_{i,\mathrm{d}}$ are the charging and discharging efficiencies of BESS.

6) The trading price constraint:

$$\rho^t_{\mathrm{b}} \leqslant \rho^t_{ij} \leqslant \rho^t_{\mathrm{s}} \tag{33}$$

b) Asymmetric Nash Bargaining Model

In Nash bargaining, all players improve their payoffs compared with the situation without cooperation (namely, disagreement points), while players with same objective functions and disagreement points have the same payoffs [27].

Standard Nash bargaining problem (NBP):

$$\begin{cases} \max\prod_{i=1}^{M}\left[C^{\mathrm{Non}}_i - C^{\mathrm{C}}_i\right] \\ \text{s.t. } C^{\mathrm{Non}}_i - C^{\mathrm{C}}_i \geqslant 0,\ (27)-(33) \end{cases} \tag{34}$$

where C^{Non}_i denotes the cost at the disagreement point without considering P2P trading; C^{C}_i is the objective function of MG$_i$ in energy trading with other MGs. The Nash bargaining model can be decomposed into two subproblems: the social cost minimization problem (P1) and the payment bargaining problem (P2), which can be solved in turn. The proof procedure for the equivalent transformation is provided in Appendix A.

$$\text{Let}: U^{\mathrm{C}}_i = C^{\mathrm{N}}_i + C^{\mathrm{net}}_i \tag{35}$$

P1: Social cost minimization subproblem is shown by

$$\begin{cases} \min\ \sum_{i=1}^{M}U^{\mathrm{C}}_i \\ \text{s.t. } (27)-(32) \end{cases} \tag{36}$$

In asymmetric Nash bargaining, an exponential function defined as energy mapping function is exploited to quantify the bargaining capability of MGs based on their contributions during P2P trading. Assuming the contribution of providing energy is larger than receiving energy, the larger the contribution MG$_i$ has, the larger bargaining value D$_i$ gains.

$$D_i = \mathrm{e}^{E^{\mathrm{supply}}_i / E^{\mathrm{supply}}_{\max}} - \mathrm{e}^{-\left(E^{\mathrm{receive}}_i / E^{\mathrm{receive}}_{\max}\right)} \tag{37}$$

$$E^{\mathrm{receive}}_i = -\sum_{t=1}^{T}\min(0, P^t_{ij}) \tag{38}$$

$$E^{\mathrm{supply}}_i = \sum_{t=1}^{T}\max(0, P^t_{ij}) \tag{39}$$

where E^{receive}_i and E^{supply}_i are the power MG$_i$ receives and provides during P2P trading, respectively.

According to (37)–(39), the optimal trading power obtained in P1 is substituted into NBP, thus the asymmetric payment bargaining model can be rewritten as:

$$\begin{cases} \max\prod_{i=1}^{M}\left[C^{\mathrm{Non}}_i - U^{\mathrm{C}*}_i - C^{\mathrm{P2P}}_i(\rho^t_{ij}, P^{t*}_{ij})\right]^{D_i} \\ \text{s.t. } C^{\mathrm{Non}}_i - U^{\mathrm{C}*}_i - C^{\mathrm{P2P}}_i(\rho^t_{ij}, P^{t*}_{ij}) > 0, \text{ and } (33) \end{cases} \tag{40}$$

The variable labeled with '∗' is the optimal solution of P1. Taking the logarithm of (40), the max can be converted into a min problem.

P2: Payment bargaining subproblem

$$\begin{cases} \min \left\{ -D_i \sum_{i=1}^{M} \ln\left[C_i^{\text{Non}} - U_i^{\text{C}*} - C_i^{\text{P2P}}(\rho_{ij}^t, P_{ij}^{t*}) \right] \right\} \\ \text{s.t. } C_i^{\text{Non}} - U_i^{\text{C}*} - C_i^{\text{P2P}}(\rho_{ij}^t, P_{ij}^{t*}) > 0, \text{ and (33)} \end{cases} \tag{41}$$

B. Intra-day Scheduling

In this section, each MGO optimizes the interactive power to ADN according to the flexibility demand issued by DSO with the objective of total operation cost minimization.

$$\min F_{\text{MMG}} = \sum_{i=1}^{M} F_{\text{MG}i}(P_{\text{MG}i}^t) \tag{42}$$

$$\sum_{i=1}^{M} P_{\text{MG}i}^t = P_{\text{D}}^t \tag{43}$$

where $F_{\text{MG}i}$ is the operating cost of MG$_i$; $P_{\text{MG}i}^t$ is the interactive power with ADN which is positive when power flows to AND; and P_{D}^t is the flexibility demand from DSO.

As stated in [28], $F_{\text{MG}i}$ can usually be expressed in a quadratic form similar to that of a conventional generation unit. The simplification is adopted to satisfy the fast response to the DSO flexibility demand.

IV. The Solution and Algorithm

A. Fuzzy Multi-objective Optimization

The multi-objective optimization model of MGs in day-ahead scheduling can be transformed as a single-objective optimization by constructing fuzzy membership function:

$$\varphi_s = \begin{cases} 1, f_s \leqslant f_s^{\min} \\ \dfrac{f_s^{\max} - f_s}{f_s^{\max} - f_s^{\min}}, f_s^{\min} < f_s < f_s^{\max} \\ 0, f_s \geqslant f_s^{\max} \end{cases} \tag{44}$$

where φ_s is the fuzzy affiliation function; f_s is the sth objective function; $f_s^{\min}$ and $f_s^{\max}$ are the minimum and maximum value of f_s respectively.

Weighting factors can be assigned based on the following:

$$\psi = \begin{cases} \sum_{s=1}^{S} \omega_s \varphi_s \\ \sum_{s=1}^{S} \omega_s = 1 \end{cases} \tag{45}$$

where S is the number of objective functions f_s; and ω_s is the satisfaction weighting factor of f_s.

B. Decentralized ADMM Solution for Nash Bargaining

1) Solving P1 (Social Cost Minimization)

Since P1 contains coupling variables for energy trading, auxiliary variables are introduced to decouple them, as:

$$P_{ij}^t = -P_{ji}^t (i, j \in \mathcal{M}, i \neq j) \tag{46}$$

Based on ADMM, the augmented Lagrange function of MG$_i$ with respect to P1 can be expressed as:

$$\begin{aligned} &\min L_{i,1}(P_{ij}^t, P_{ji}^t, \lambda_{ij,\text{P1}}^t) = U_i^{\text{C}} - \\ &\sum_{t=1}^{T} \sum_{j \in \mathcal{M}/i} \left(\frac{\rho_1}{2} \left\| P_{ij}^t + P_{ji}^t \right\|_2^2 + \lambda_{ij,\text{P1}}^t (P_{ij}^t + P_{ji}^t) \right) \end{aligned} \tag{47}$$

where ρ_1 and $\lambda_{ij,\text{P1}}^t$ are the penalty parameter and Lagrange multiplier of P1, respectively. MG$_i$ repeats the steps in (48) until the iterative convergence is met in (49).

$$\begin{cases} P_{ij}^t(k+1) = \arg\min\limits_{P_{ij}^t(k)} L_{i,1}(P_{ij}^t(k), P_{ji}^t(k), \lambda_{ij,\text{P1}}^t(k)) \\ P_{ji}^t(k+1) = \arg\min\limits_{P_{ji}^t(k)} L_{j,1}(P_{ij}^t(k+1), P_{ji}^t(k), \lambda_{ji,\text{P1}}^t(k)) \\ \lambda_{ij,P1}^t(k+1) = \lambda_{ij,P1}^t(k) + \rho_1 (P_{ij}^t(k+1) + P_{ji}^t(k+1)) \end{cases} \tag{48}$$

$$\begin{aligned} &\sum_{t=1}^{T} \sum_{j \in \mathcal{M}/i} \left\| P_{ij}^t(k) + P_{ji}^t(k) \right\|_2 \leqslant \varepsilon_{\text{r},1} \\ &\sum_{t=1}^{T} \sum_{j \in \mathcal{M}/i} \left\| P_{ij}^t(k+1) - P_{ij}^t(k) \right\|_2 \leqslant \varepsilon_{\text{d},1} \end{aligned} \tag{49}$$

where k is the number of iterations; while $\varepsilon_{\text{r},1}$ and $\varepsilon_{\text{d},1}$ are the convergence thresholds of primal and dual residuals, respectively.

2) Solving P2 (Payment Bargaining)

Similarly, auxiliary variables are introduced since P2 contains coupling variables for the trading price, as:

$$\rho_{ij}^t = \rho_{ji}^t (i, j \in \mathcal{M}, \ i \neq j) \tag{50}$$

The augmented Lagrange function of MG$_i$ with respect to P2 can be expressed as:

$$\begin{aligned} &\min L_{i,2}(\rho_{ij}^t, \rho_{ji}^t, \lambda_{ij,\text{P2}}^t) = \\ &-D_i \ln\left(C_i^{\text{Non}} - U_i^{\text{C}*} - C_i^{\text{P2P}}(\rho_{ij}^t, P_{ij}^{t*}) \right) - \\ &\sum_{i=1}^{T} \sum_{j \in \mathcal{M}/i} \left[\frac{\rho_2}{2} \left\| \rho_{ij}^t - \rho_{ji}^t \right\|_2^2 + \lambda_{ij,\text{P2}}^t (\rho_{ij}^t - \rho_{ji}^t) \right] \end{aligned} \tag{51}$$

where ρ_2 and $\lambda_{ij,\text{P2}}^t$ are the penalty parameter and Lagrange multiplier of P2. MG$_i$ repeats the steps in (52) until the iterative convergence is met in (53).

$$\begin{cases} \rho_{ij}^t(k+1) = \arg\min\limits_{\rho_{ij}^t(k)} L_{i,1}(\rho_{ij}^t(k), \rho_{ji}^t(k), \lambda_{ij,\text{P2}}^t(k)) \\ \rho_{ji}^t(k+1) = \arg\min\limits_{\rho_{ji}^t(k)} L_{j,1}(\rho_{ij}^t(k+1), \rho_{ji}^t(k), \lambda_{ji,\text{P2}}^t(k)) \\ \lambda_{ij,\text{P2}}^t(k+1) = \lambda_{ij,\text{P2}}^t(k) + \rho_2 (\rho_{ij}^t(k+1) - \rho_{ji}^t(k+1)) \end{cases} \tag{52}$$

$$\begin{cases} \sum_{t=1}^{T}\sum_{j\in\mathcal{M}/i}\left\|\rho_{ij}^{t}(k)-\rho_{ji}^{t}(k)\right\|_2 \leqslant \varepsilon_{\mathrm{r},2} \\ \sum_{t=1}^{T}\sum_{j\in\mathcal{M}/i}\left\|\rho_{ij}^{t}(k+1)-\rho_{ij}^{t}(k)\right\|_2 \leqslant \varepsilon_{\mathrm{d},2} \end{cases} \tag{53}$$

where $\varepsilon_{\mathrm{r},2}$ and $\varepsilon_{\mathrm{d},2}$ are the convergence thresholds of primal and dual residuals, respectively.

The coefficient τ is introduced to adjust the penalty parameter to reconcile the primal residuals r_a with the dual residuals d_a.

$$\rho_a^{k+1}=\begin{cases} \tau\rho_a^k, & r_a^k>\mu_{\mathrm{r}}d_a^k \\ \rho_a^k/\tau, & r_a^k<\mu_{\mathrm{r}}d_a^k \\ \rho_a^k, & \text{other} \end{cases} \quad (a=1,2) \tag{54}$$

where μ_{r} represents the multiple of the difference between the primal and dual residuals.

The flowchart of the ADMM-based Nash bargaining model is shown in Fig. 3.

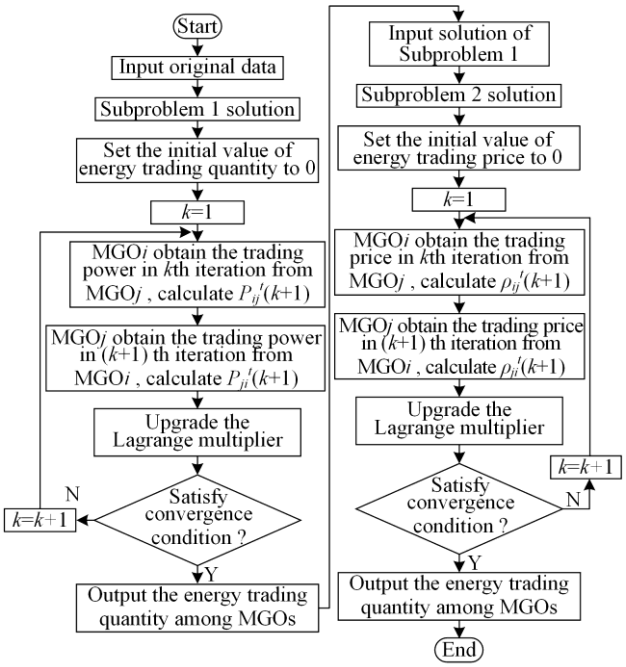

Fig. 3. Flowchart of the proposed ADMM-based Nash bargaining model.

C. Average Consensus Based Decentralized Newton Method

1) Outer Level: Decentralized Newton Algorithm

According to [29], equation (42) is feasible with a convex objective function F_{MMG} and a finite optimal value. Given an initial feasible vector $\boldsymbol{P}_{\mathrm{MG}}^0$ which is strictly positive, the algorithm generates the iteration by:

$$\boldsymbol{P}_{\mathrm{MG}}^{k+1}=\boldsymbol{P}_{\mathrm{MG}}^{k}+d^k\Delta\boldsymbol{P}_{\mathrm{MG}}^{k} \tag{55}$$

where d^k is the iteration step size at step k; $\boldsymbol{P}_{\mathrm{MG}}^k$ is the interactive power vector as well as Newton primal vector; and $\Delta\boldsymbol{P}_{\mathrm{MG}}^k$ is the Newton direction given as the solution of the following linear equations:

$$\begin{bmatrix} \nabla^2\boldsymbol{F}(\boldsymbol{P}_{\mathrm{MG}}^k) & \boldsymbol{e}_{\mathrm{m}} \\ \boldsymbol{e}_{\mathrm{m}}^{\mathrm{T}} & 0 \end{bmatrix}\begin{bmatrix} \Delta\boldsymbol{P}_{\mathrm{MG}}^k \\ \boldsymbol{w}^k \end{bmatrix}=-\begin{bmatrix} \nabla\boldsymbol{F}(\boldsymbol{P}_{\mathrm{MG}}^k) \\ 0 \end{bmatrix} \tag{56}$$

where $\boldsymbol{e}_{\mathrm{m}}$ is the 1 vector of size M; $\boldsymbol{w}^k$ is the Newton dual vector; and $\boldsymbol{H}_k=\nabla^2\boldsymbol{F}(\boldsymbol{P}_{\mathrm{MG}}^k)$ denotes the Hessian matrix of $\boldsymbol{P}_{\mathrm{MG}}^k$ for notational convenience. Equation (56) can be rewritten as:

$$\Delta\boldsymbol{P}_{\mathrm{MG}}^k=-\boldsymbol{H}_k^{-1}(\nabla\boldsymbol{F}(\boldsymbol{P}_{\mathrm{MG}}^k)+\boldsymbol{e}_{\mathrm{m}}\boldsymbol{w}^k) \tag{57}$$

$$(\boldsymbol{e}_{\mathrm{m}}^{\mathrm{T}}\boldsymbol{H}_k^{-1}\boldsymbol{e}_{\mathrm{m}})\boldsymbol{w}^k=-\boldsymbol{e}_{\mathrm{m}}^{\mathrm{T}}\boldsymbol{H}_k^{-1}\nabla\boldsymbol{F}(\boldsymbol{P}_{\mathrm{MG}}^k) \tag{58}$$

Since the operating cost of each MG depends only on the interaction power with DSO, $\boldsymbol{H}_k$ and $\nabla\boldsymbol{F}(\boldsymbol{P}_{\mathrm{MG}}^k)$ have a special form which enables the inverse process of $\boldsymbol{H}_k$ and $\nabla\boldsymbol{F}(\boldsymbol{P}_{\mathrm{MG}}^k)$ calculated in a decentralized manner.

$$\boldsymbol{H}_k=\mathrm{diag}\left\{H_{k,11},H_{k,22},\cdots,H_{k,ii}\right\} \tag{59}$$

$$H_{k,ii}=\frac{\partial^2 F_{\mathrm{MG}i}(\boldsymbol{P}_{\mathrm{MG}i}^k)}{\partial(\boldsymbol{P}_{\mathrm{MG}i}^k)^2} \tag{60}$$

The ith element of $\nabla\boldsymbol{F}(\boldsymbol{P}_{\mathrm{MG}}^k)$ is:

$$\nabla\boldsymbol{F}_i(\boldsymbol{P}_{\mathrm{MG}}^k)=\frac{\mathrm{d}F_{\mathrm{MG}i}(\boldsymbol{P}_{\mathrm{MG}i}^k)}{\mathrm{d}\boldsymbol{P}_{\mathrm{MG}i}^k} \tag{61}$$

Equations (55)–(58) can be rewritten as:

$$\boldsymbol{P}_{\mathrm{MG}i}^{k+1}=\boldsymbol{P}_{\mathrm{MG}i}^{k}+d^k\Delta\boldsymbol{P}_{\mathrm{MG}i}^{k} \tag{62}$$

$$\Delta\boldsymbol{P}_{\mathrm{MG}i}^k=-H_{k,ii}^{-1}(\nabla\boldsymbol{F}_i(\boldsymbol{P}_{\mathrm{MG}}^k)+\boldsymbol{w}^k) \tag{63}$$

$$\boldsymbol{w}^k=-\frac{\sum_{i=1}^{M}H_{k,ii}^{-1}\nabla\boldsymbol{F}_i(\boldsymbol{P}_{\mathrm{MG}}^k)}{\sum_{i=1}^{M}H_{k,ii}^{-1}} \tag{64}$$

As shown in (60) and (61), $H_{k,ii}$ and $\nabla\boldsymbol{F}_i(\boldsymbol{P}_{\mathrm{MG}}^k)$ can be acquired totally by local information of MG_i. MG_i needs to exchange $H_{k,ii}^{-1}$ and $H_{k,ii}^{-1}\nabla\boldsymbol{F}_i(\boldsymbol{P}_{\mathrm{MG}}^k)$ between neighbors to obtain common variables $\boldsymbol{w}^k$ according to the average consensus algorithm.

$$\sum H_{k,ii}^{-1}=Mf_{\mathrm{ave}}(H_{k,ii}^{-1}) \tag{65}$$

$$\sum H_{k,ii}^{-1}\nabla\boldsymbol{F}_i(\boldsymbol{P}_{\mathrm{MG}}^k)=Mf_{\mathrm{ave}}(H_{k,ii}^{-1}\nabla\boldsymbol{F}_i(\boldsymbol{P}_{\mathrm{MG}}^k)) \tag{66}$$

2) Inner Level: Average Consensus Algorithm

Let $\mathcal{G}=(E,V)$ denote an undirected graph with vertex set $V=\{1,2,\ldots,M\}$ and edge set $E=\{\{i,j\}|i,j\in V\}$. Let $\mathcal{N}_i=\{j\in V|\{i,j\}\in E\}$ denotes the neighbor set of node i. Each edge on the graph represents the communication connection relationship between MG nodes.

At each iteration step h, each node updates its state $x_i(h)$:

$$x_i(h+1)=W_{ii}x_i(h)+\sum_{j\in\mathcal{N}_i}W_{ij}x_j(h),\quad i=1,\cdots,M \tag{67}$$

where W_{ij} is the linear weighting on $x_j(h)$ at node i. Set $W_{ij}=0$ for $j \notin \mathcal{N}_i$, the weighting matrix $\boldsymbol{W} \in R^{M\times M}$ can be determined by metropolis algorithm in [30].

All nodes reach consensus if and only if $x_i = x_j$ for all $i, j \in \{1,2,\cdots,M\}$. A consensus algorithm establishes a mapping $\chi: R^M \to R$ converging all elements of vector x to a value x^*:

$$x^* = f_{\text{ave}}(\boldsymbol{x}) = \frac{1}{M}\sum_{i=1}^{M} x_i \tag{68}$$

The flowchart of the proposed average consensus-based decentralized Newton method is shown in Fig. 4.

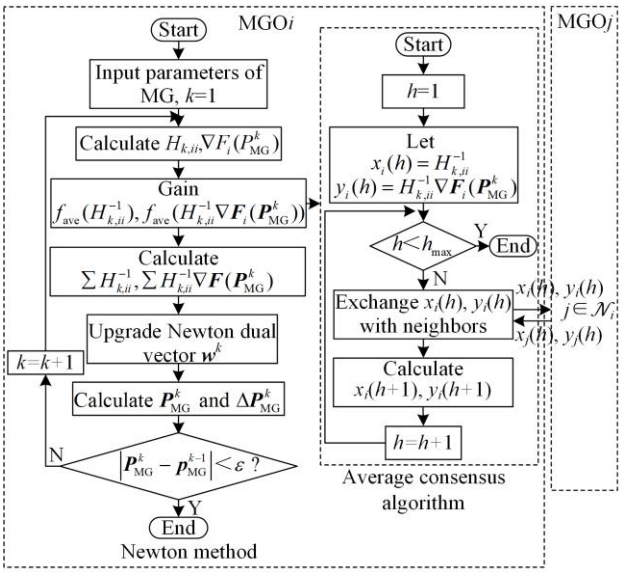

Fig. 4. Flowchart of the average consensus-based decentralized Newton method.

V. Case Study

A. Parameters

Figure 5 shows the schematic network structure of a regional ADN with MMGs.

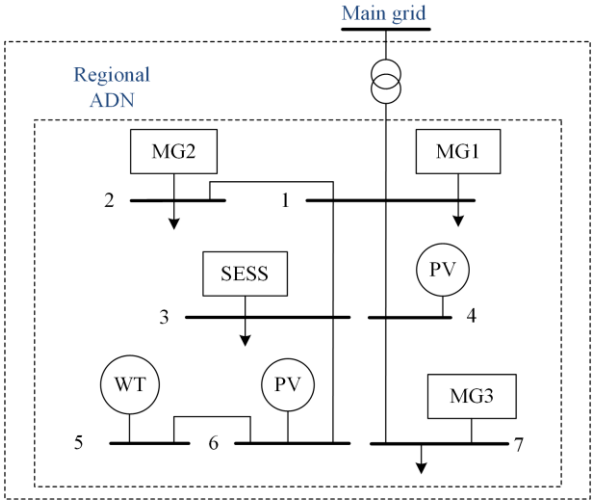

Fig. 5. Schematic network structure of a regional ADN with MGs.

MG_1 is located in the area with rich PV installation. MG_2 and MG_3 represent the areas with high penetration of wind power, while MG_2 is also installed with small-scale PV. It is assumed that they have the same equipment parameters. The tariff of the main grid is 0.093 \$/kWh, purchase price set by ADN is assumed to remain unchanged as 0.043 \$/kWh, and $\overline{\rho}_{\text{s·max}}$ is 0.11 \$/kWh. The typical daily REs and load profiles of the case study network and the parameters of MGs are shown in Appendix B. The RE generation at intra-day stage with boundaries of uncertainties are shown in Appendix C.

B. Scheduling Results at Day-ahead Stage

1) Charging and Discharging Strategies of SESS

Figure 6 shows the daily charging/discharging strategies and the associate SOC variations of the SESS. It can be seen that SESO implements the power interaction with ADN for profit after meeting leasing demands of MGs.

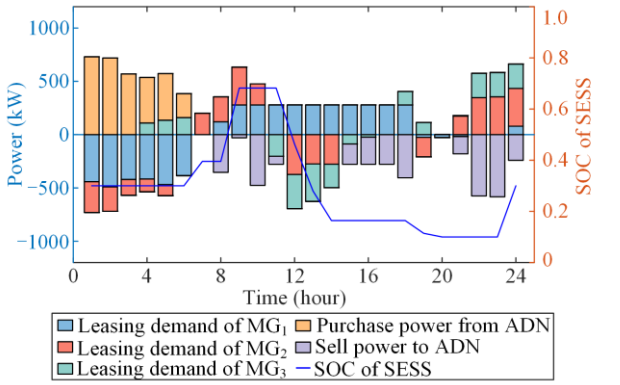

Fig. 6. Charging/discharging strategies and SOC variations of SESS.

The operation cost of SESS is \$73.56 in response to the TOU price, while it is \$169.73 when only meets the leasing demands. Therefore, the introduction of TOU price is economically feasible for SESS.

2) Leasing Strategies of MGOs

Let the satisfaction weighting $w_1 = 0.4$ and $w_2 = 0.6$, Table II shows the comparison of the net load mean squared deviation and leasing cost of MGs. Figure 7 shows the leasing demands of MGOs and the comparison of the net load profiles before and after smoothing the fluctuations. It can be seen that all MGs have smoothed the net load fluctuations to some extent by leasing SESS.

TABLE II
Multi-objective Optimization Results for MGs

MGs	Leasing cost (\$)	Net load mean squared deviation before leasing (kW^2)	Net load mean squared deviation after leasing (kW^2)
MG_1	181.92	9.42×10^6	4.99×10^6
MG_2	165.33	3.44×10^6	7.62×10^5
MG_3	158.65	6.83×10^6	4.41×10^6

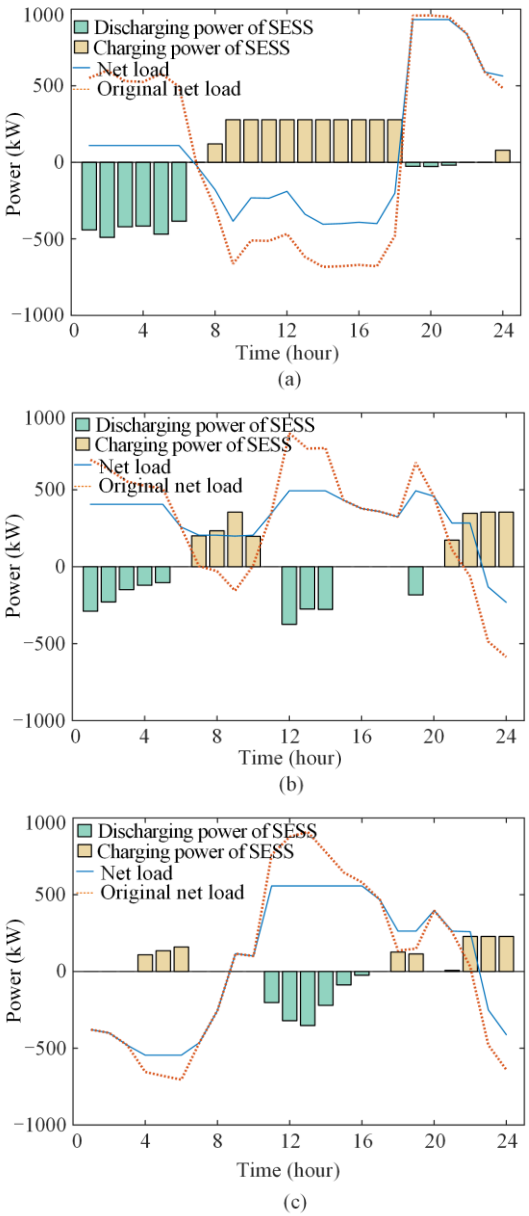

Fig. 7. SESS leasing demands from MGs. (a) SESS leasing demand from MG_1. (b) SESS leasing demand from MG_2. (c) SESS leasing demand from MG_3.

3) Nash Bargaining Results Among MGs

a) P2P Trading Strategies

The energy trading results of MGs under cooperative operation are shown in Fig. 8 and Fig. 9. Taking MG_1 as an example, in order to smooth the fluctuations, MG_1 leases SESS to compensate the power shortage at 1:00–6:00 and a small amount of electricity is purchased from DSO during this time. During 8:00–18:00, with excessive PV access, MG_1 leases SESS to support part of the load while also sells energy to MG_2 and MG_3 to achieve revenue. In particular, during 11:00–18:00, MG_1 increases the energy production from MT to provide energy support to other MGs. From 19:00–21:00, MG_1 has insufficient power supply due to the increase of demand so prioritizes energy purchase from other MGs to reduce the operation cost using local FRs. The BESS within MG_1 is mainly charged at flat and off-peak hours and discharged at peak hours to reduce operation cost. Demand response allows the load in peak hours to be shifted to off-peak hours to a certain extent, relieving the supply pressure on the MGO.

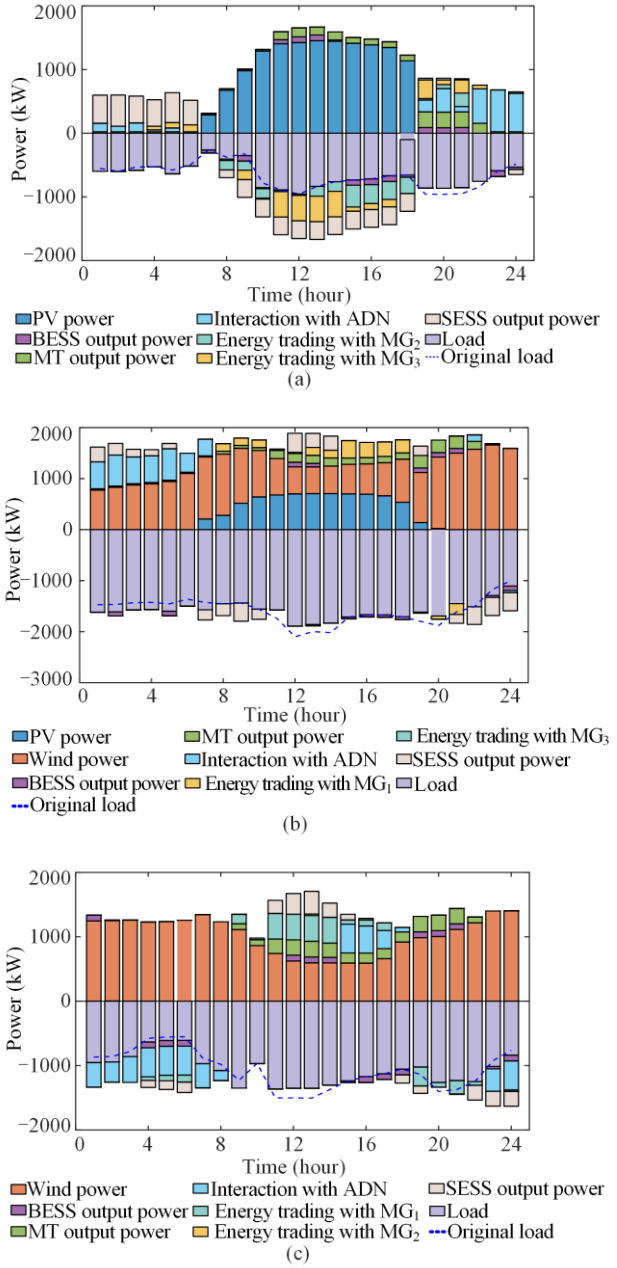

Fig. 8. Scheduling results of MGs under cooperative operation. (a) Scheduling result of MG_1. (b) Scheduling result of MG_2. (c) Scheduling result of MG_3.

It can be seen from Fig. 9 that at day-ahead stage, the amount of energy trading among MGs is in balanced condition. The trading price is lower than the TOU sale price and higher than the purchase price of DSO at all time periods, which means power-selling MGs can obtain more profit while the power-purchasing MGs can reduce the cost through P2P trading.

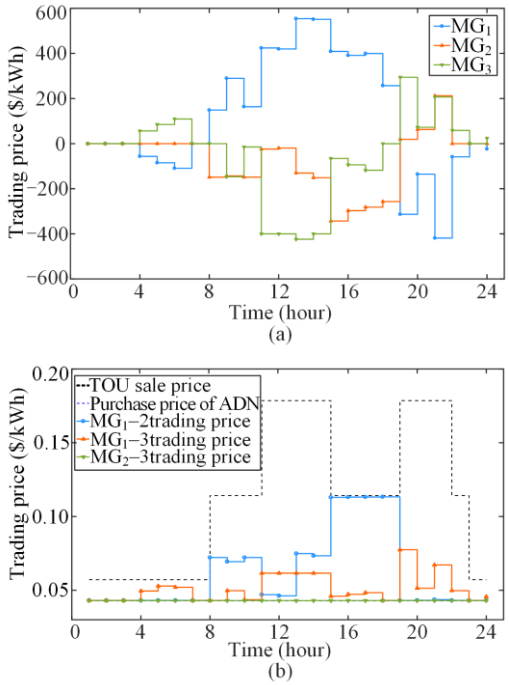

Fig. 9. Trading results among MGs. (a) Energy trading quantity. (b) Energy trading price.

b) Revenue and Cost Analysis

Table III and Table IV summary the revenues and costs of MGs in asymmetric and symmetric Nash bargaining, respectively. In Table IV, the total cost of each MG decreases by \$97.55, \$97.56, and \$97.56, which are almost identical. However, the allocations are clearly unfair due to different power contributions of MGs. In asymmetric Nash bargaining, MG_1 is mainly selling energy, the higher asset utilization leads to a slight increase in operation cost during the bargaining transaction, while the revenue is positive. MG_2 and MG_3 are mainly purchasing energy to reduce the operation costs while the revenues of the trading are negative. Comparing to MG_2 and MG_3, MG1 has a larger energy contribution value, namely, a larger asymmetric bargaining factor of 2.1595, tending to receive more cooperative benefits.

The total cost of each MG decreases by \$168.08, \$54.57 and \$69.30, with the cost reduction ratio of 57.69%, 18.64% and 23.67%, respectively. The benefits of all participants are effectively and fairly improved.

TABLE III
REVENUE AND COSTS IN ASYMMETRIC NASH BARGAINING

MGs	Asymmetric bargaining factor	Operation cost with P2P trading ($)	Revenue in Nash bargaining ($)	Total cost with P2P trading ($)	Total cost without P2P trading ($)	Revenue improvement value ($)	Daily power contribution (kW)
MG_1	2.1595	537.06	238.89	298.97	467.05	168.08	2807.07
MG_2	0.6974	514.88	−175.58	690.46	745.03	54.57	−1650.76
MG_3	0.8860	321.79	−63.20	384.99	454.29	69.30	−1156.49

TABLE IV
REVENUE AND COST IN SYMMETRIC NASH BARGAINING

MGs	Revenue in Nash bargaining ($)	Total cost with P2P trading ($)	Revenue improvement ($)
MG_1	167.56	369.50	97.55
MG_2	−132.59	647.47	97.56
MG_3	−34.94	356.73	97.56

c) Flexibility Analysis

To analyze the impact of MGs and SESS participation in providing flexibility, three scenarios are designed for comparison:

Scenario 1: MGs only trade with ADN.

Scenario 2: Flexibility is only provided by SESS without considering the P2P trading among MGs.

Scenario 3: Flexibility is provided by both SESS and MGs.

Figure 10 shows the energy transactions between MGs and ADN under the three scenarios. It can be seen that each MG reduces the dependence with ADN. The consumption level of REs in each MG is increased from 89%, 99.85%, 97.80%, respectively to 100% by P2P flexibility trading and SESS leasing strategies.

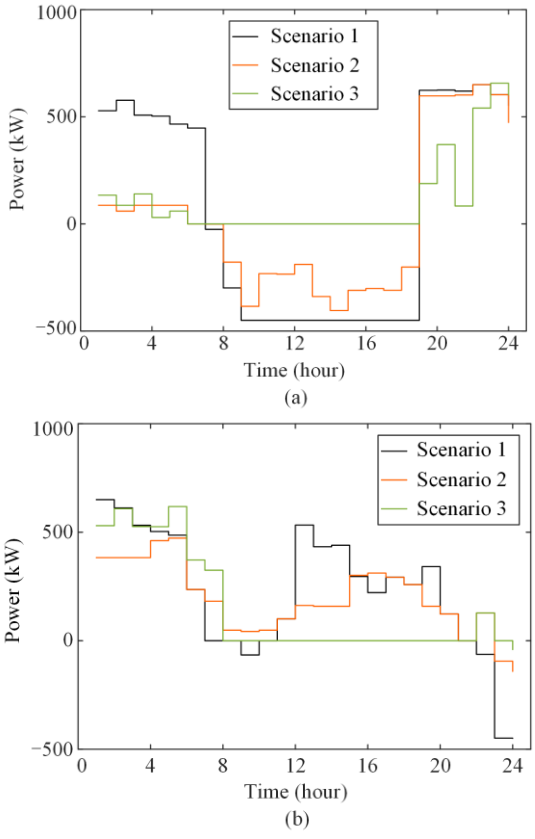

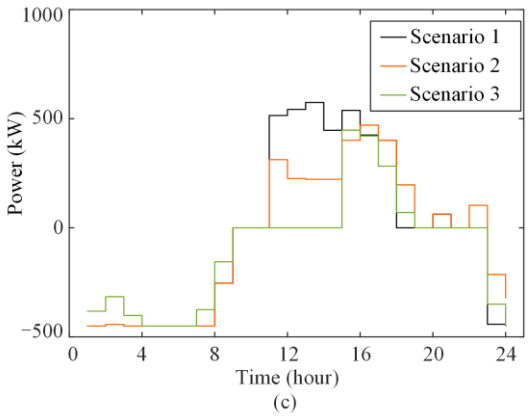

Fig. 10. Energy interaction between MGs and ADN. (a) Energy interaction between MG_1 and ADN. (b) Energy interaction between MG_2 and ADN. (c) Energy interaction between MG_3 and ADN.

4) Convergence Analysis

The iterative convergence process of subproblem 1 and subproblem 2 in P2P trading is shown in Appendix C. The ADMM algorithm has demonstrated good convergence performance and computation efficiency. The total cost of each MG is \$298.97, \$690.46, \$384.99 when the algorithm converges. A typical heuristic algorithm, namely, differential evolution algorithm [31], is utilized in Stackelberg game of DSO and other participants. The optimization iterative process of DSO is also shown in Appendix D.

C. Scheduling Results at Intra-day Stage

The operation cost of each MG is assumed to be a quadratic function with respect to the interactive power, and the cost coefficients a_{Mi}, b_{Mi}, c_{Mi} of MT are used to represent the coefficients of the quadratic, linear, and constant terms of the cost function, respectively.

Figure 11 shows the flexibility supply results of MGs during the day in response to the rapid flexibility demand of DSO. The flexibility services are provided jointly by all MGs with their power adjustability. MG_1 provides the maximum percentage of flexibility output since it has the lowest operation cost.

Figure 12 shows the cost increment rate of MGs at each time when the algorithm reaches convergence. The proposed algorithm achieves the minimum regulation cost based on the equal cost increment rate criteria, which means the total generation cost achieves a minimum value when the generation cost increments for all generators are equal. The computation time for 96 slots and the power output variations of MGs at time slot t=37 is shown in Fig. 13. This result illustrates that the consensus-based decentralized Newton method is computationally effective due to the second order gradient information of Hessian matrix.

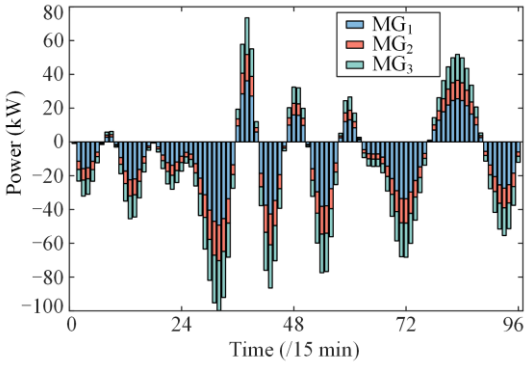

Fig. 11. Results of MGs in response to the flexibility demand (every 15 minutes of 1 day).

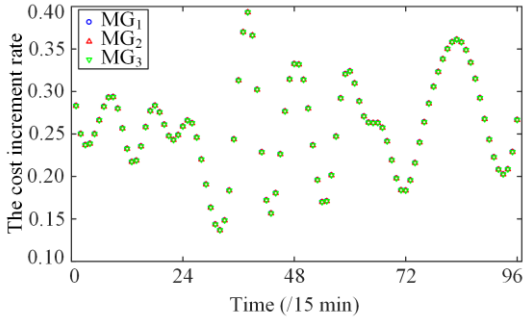

Fig. 12. The cost increment rate of MGs (every 15 minutes of 1 day).

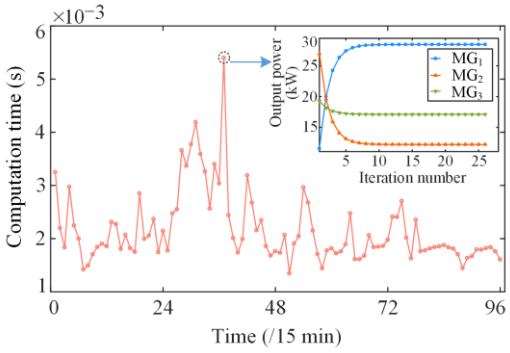

Fig. 13. The computation time and associate convergence under worst computation case of decentralized Newton method (every 15 minutes of 1 day).

In order to verify the effectiveness of the second-order distributed Newton method proposed in this paper, a representative sub-gradient algorithm of the first-order distributed algorithms is chosen as a benchmark. Figure 14 shows the iteration number when the two algorithms reach convergence for the three MGs. Both algorithms yield essentially the same optimal value but with different convergence times. As seen, it only needs about 20 iterations utilizing the decentralized Newton method, compared to more than 40 iterations with the sub-gradient algorithm. This result illustrates that the decentralized Newton method proposed in this paper significantly improves the convergence speed compared to the traditional first-order one due to the utilization of the second-order gradient information. It satisfies the requirements of algorithmic flexibility and efficiency, and such effect can be more significant in larger scale systems.

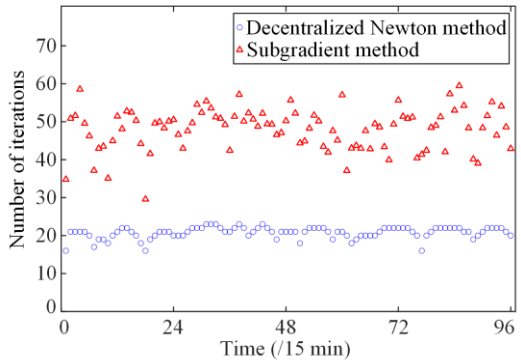

Fig. 14. The comparison of iterations for two algorithms.

For a larger system, i.e., M=6, the iteration numbers for the two algorithms to reach convergence are shown in Fig. 15. It can be seen that in a larger scale system, there is a significant increase in the iteration number for the sub-gradient algorithm compared to the smaller system. The average iteration number is around 95, while the average iteration number of the decentralized Newton method does not increase significantly. In addition, the iteration number of the decentralized Newton algorithm is largely unchanged under different communication densities between MGs, which reflects the advantage in computational stability.

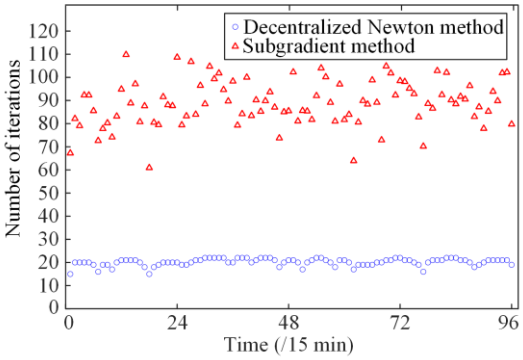

Fig. 15. The comparison of iterations of two algorithms for larger scale system.

To summarize, in a larger scale system, the decentralized Newton method is less susceptible to the influence of the number and the communication density of the participants, so can better meet the requirements for algorithmic efficiency and stability in practical applications.

VI. Conclusion

A two-stage coordinated flexibility trading mechanism is developed in this paper to further release the flexibility from distribution system and explore the potential flexibility of DERs. The hierarchical framework of flexibility trading with multiple types of FRs at various time scales can smooth the power fluctuations brought by the high proliferation of REs, and enhance the overall system flexibility. The proposed asymmetric Nash bargaining approach can provide executable solutions in maximizing social benefit while guaranteeing fair revenue allocation simultaneously. The proposed decentralized algorithms can provide super-linear convergence while ensuring the privacy of each participant and addressing the rapid response requirements on flexibility.

Appendix A

It is clear that the following equation needs to be satisfied when (34) obtains its maximum value:

$$\prod_{i=1}^{M}\left[C_i^{\mathrm{Non}}-C_i^{\mathrm{C}}\right]=\left[\frac{1}{M}\sum_{i=1}^{M}(C_i^{\mathrm{Non}}-C_i^{\mathrm{C}})\right]^{M} \tag{A1}$$

Since the benefit received by the power-selling MG is equal to the cost of the power-purchasing MG when operators trade energy with each other, then:

$$\sum_{i=1}^{M}C_i^{\mathrm{P2P}}=0 \tag{A2}$$

Let $U_i^{\mathrm{C}}=U_i^{\mathrm{N}}+U_i^{\mathrm{net}}$, then the objective function is:

$$\max\left\{M\ln\left[\frac{1}{M}\sum_{i=1}^{M}(C_i^{\mathrm{Non}}-U_i^{\mathrm{C}})\right]\right\} \tag{A3}$$

Since C_i^{Non} is a constant without cooperative energy trading, the objective function is transformed as:

$$\min\ \sum_{i=1}^{M}U_i^{\mathrm{C}} \tag{A4}$$

Therefore, equation (34) is transformed into a social cost minimization problem P1.

P1: Social cost minimization subproblem:

$$\begin{cases}\min\ \sum_{i=1}^{M}U_i^{\mathrm{C}}\\ \text{s.t. } (27)-(32)\end{cases} \tag{A5}$$

Appendix B

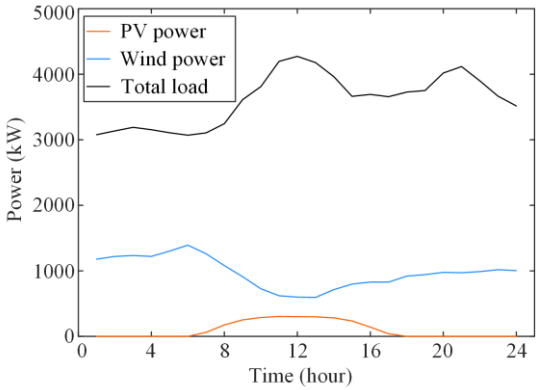

Fig. B1. REs and load profiles of ADN.

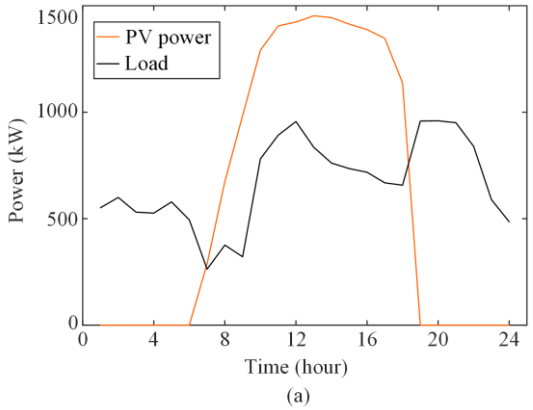

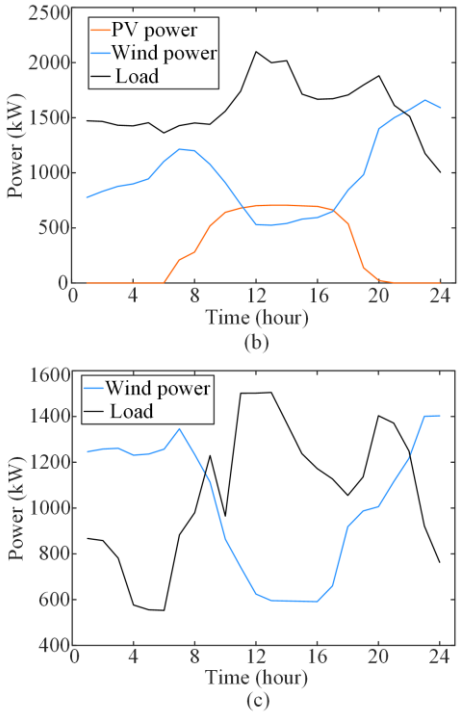

Fig. B2. REs and load profile of MGs. (a) REs and load profile of MG_1. (b) REs and load profile of MG_2. (c) REs and load profile of MG_3.

TABLE BI
THE PARAMETERS OF MGS

Parameter	Value	Parameter	Value
ζ_b (\$/kW)	0.0021	$\alpha_{i,\text{tran}}$	0.1
λ_e^{tran} (\$/kW)	0.0286	$\eta_{i,c}, \eta_{i,d}$	95%
a_{Mi} (\$/kW^2)	0.000 21	$P_{i,\text{Bch}}^{\max}$ (kW)	90
b_{Mi} (\$/kW)	0.0473	$P_{i,\text{Bdis}}^{\max}$ (kW)	90
c_{Mi} (\$)	0.75	$S_i^{\min}$ (kWh)	80
$P_{\text{grid}}^{\max}$ (kW)	650	$S_i^{\max}$ (kWh)	360
$P_{\text{MT}}^{\min}$ (kW)	0	γ_1^e (\$/kW^2)	0.000 03
$P_{\text{MT}}^{\max}$ (kW)	245	γ_2^e (\$/kW)	0.0014
θ_i	0.01		

TABLE BII
THE PARAMETERS OF SESS

Parameter	Value	Parameter	Value
u (\$/kWh)	0.058	ζ_s (\$/kW)	0.022
v (\$/kWh)	0.204	μ_s	0.1
w (\$/kWh)	0.022	$E_{\text{SESS}}^{\max}$ (kWh)	2000
α_{Lea}	1.2	$P_{\text{SESS}}^{\max}$ (kW)	1000
η_c (%)	95	η_d (%)	95

TABLE BIII
THE PARAMETERS OF ALGORITHMS

Algorithm	Parameter	Value
ADMM	Convergence threshold of P1,P2	10^{-3}, 10^{-3}
	Penalty factor of P1,P2	10^{-3}, 1
Differential evolution	Number of iterations	150
	Number of populations	30
	Crossover factor	0.9
Decentralized Newton	Iteration step size	0.5

APPENDIX C

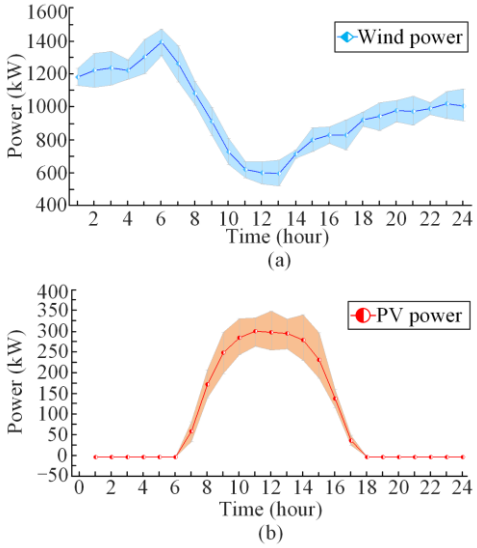

Fig. C1. Predictions at day-ahead stage. (a) Available daily wind power of AND. (b) Available daily PV power of AND.

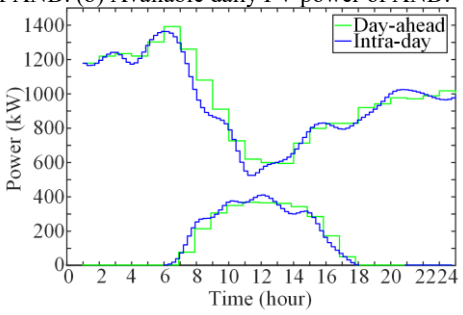

Fig. C2. Practical output at intra-day stage.

APPENDIX D

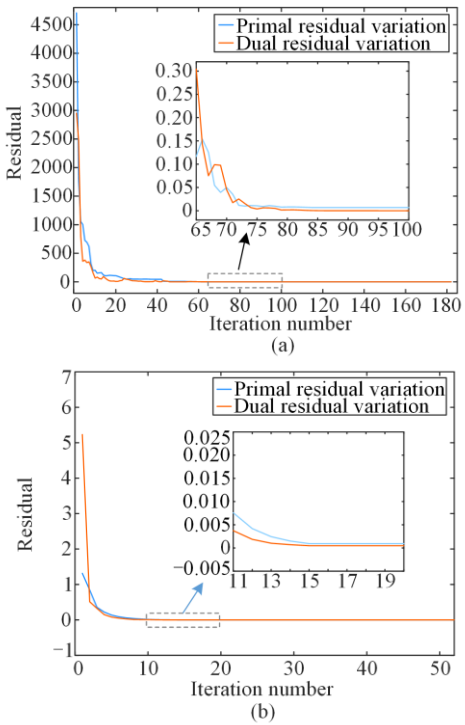

Fig. D1. Convergence results of MGs. (a) Convergence of P1. (b) Convergence of P2.

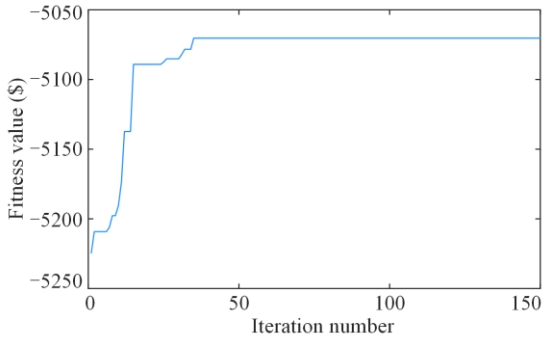

Fig. D2. The optimization iterative process of DSO.

AUTHORS' CONTRIBUTIONS

Tao Xu: conceptualization, formal analysis, funding acquisition, investigation, methodology. Rujing Wang: conceptualization, data curation, formal analysis, methodology, visualization, writing-original draft. He Meng: formal analysis, resources, validation, writing-review & editing. Mengchao Li: visualization, writing-review & editing. Hongru Wang: data curation, visualization. Yu Ji: project administration, validation. Ying Zhang: project administration. Qingrong Zheng: validation. Ping Song: project administration. Jiani Xiang: project administration. All authors read and approved the final manuscript.

FUNDING

The study is partially supported by the National Key Research & Development Program (No. 2021YFB2401204), the National Natural Science Foundation of China (No. 52277119) and the Natural Science Foundation of Tianjin Municipal (No. 22JCZDJC00690).

AVAILABILITY OF DATA AND MATERIALS

Not applicable.

DECLARATIONS

Competing interests: The authors declare that they have no known competing financial interests or personal relationships that could have appeared to influence the work reported in this paper.

AUTHORS' INFORMATION

Tao Xu received her M.S. and Ph.D. degrees from the University of Liverpool and University of Plymouth, UK, in 2004 and 2007 respectively. She joined the University of Durham, UK, as a post-doc researcher in 2007. Currently, she is an associate professor in the School of Electrical and Information Engineering, Tianjin University, China. Her research interests are centred in the area of planning, operation and control of active distribution networks with renewables.

Rujing Wang received her B.E. degree in electrical engineering from Hebei University of Technology, China, in 2021. She is currently pursuing her Ph.D. degree in electrical engineering with Tianjin University. Her research interests include planning and operation of active distribution networks with renewables and microgrids etc.

He Meng received his M.S. degree in electrical engineering from Tianjin University, China, in 2020 and he is currently pursuing his Ph.D. degree in the same institution. His research interests are mainly in optimal configuration and operation of distributed energy resources in distribution networks.

Mengchao Li received his B.Eng. degree in electrical engineering from North China Electric Power University, China, in 2020. He is currently pursuing his M.S. degree in electrical engineering with Tianjin University. His research interests include planning and operation of energy storage in distribution networks etc.

Hongru Wang received the B.Eng. degree in electrical engineering and automation from Tianjin University, China in 2022. She is currently pursuing her M.S. degree in electrical engineering with Tianjin University. Her research interests include the planning and operation of active distribution networks with a high proportion of renewable energy.

Yu Ji works at the State Grid Shanghai Energy Interconnection Research Institute Co. LTD, Shanghai, China. His research interests are distributed energy sources, microgrids and virtual power plant technology.

Ying Zhang works at the State Grid Shanghai Energy Interconnection Research Institute Co. LTD, Shanghai, China. Her research interests are optimal scheduling of distributed energy sources and virtual power plant technology.

Qingrong Zheng works at the State Grid Shanghai Municipal Electric Power Company, Shanghai, China. His research interest is the optimal scheduling of distributed energy sources.

Ping Song works at the State Grid Shanghai Municipal Electric Power Company, Shanghai, China. His research interest is related to the virtual power plant technology.

Jiani Xiang works at the State Grid Shanghai Municipal Electric Power Company, Shanghai, China. Her research interest is related to the virtual power plant technology.

REFERENCES

[1] *Energy white paper: powering our net zero future* (Dec. 2020), [Online]. Available: https://www.gov.uk/government/publications /energy-white-paper-powering-our-net-zero-future.

[2] *European Green Deal* (Dec. 2019), [Online]. Available: https://www.consilium. europa.eu/en/policies/green-deal/.

[3] *Tackling the Climate Crisis at Home and Abroad* (Jan. 2021), [Online]. Available: https://www. federalregister.gov/doc uments/ 2021/ 02 /01/2021-02177/tackling-the-climate-crisis-at-home-and-abroad.

[4] M. Qin, Y. Yang and X. Zhao *et al.*, "Low-carbon economic multi-objective dispatch of integrated energy system considering the price fluctuation of natural gas and carbon emission accounting," *Protection and Control of Modern Power Systems*, vol. 8, no. 4, pp. 1-18, Oct. 2023.

[5] *100% renewable electricity: a roadmap to 2050 for Europe and north Africa* (2010), [Online]. Available: https://www.semant icscholar. org.

[6] M. M. Hand, S. Baldwin, and E. Demeo *et al.*, "*Re-newable electricity futures study*," National Renewable Energy Laboratory, Colorado,USA, 2014.

[7] H. Gao, R. Wang, and S. He *et al.*, "Bi-level stackelberg game-based distribution system expansion planning model considering long-term renewable energy contracts," *Protection and Control of Modern Power Systems*, vol. 8, no. 4, pp. 1-15, Oct. 2023.

[8] *Power system flexibility for the energy transition* (Mar. 2022), [Online]. Available: https://www.irena. org/ publications/2018/Nov/Power-system-flexibility-for-the-energy -transition.

[9] J. Ma, V. Silva, and R. Belhomme *et al.*, "Evaluating and planning flexibility in sustainable power systems," *IEEE Transactions on Sustainable Energy*, vol. 4, no. 1, pp. 200-209, Jan. 2013.

[10] P. Das, P. Mathuria, and R. Bhakar *et al.*, "Flexibility requirement for large-scale renewable energy integration in Indian power system: technology policy and modeling options," *Energy Strategy Reviews*, vol. 29, Apr. 2020.

[11] L. Badesa, G. Strbac, and M. Magill *et al.*, "Ancillary services in Great Britain during the COVID-19 lockdown: a glimpse of the carbon-free future," *Applied Energy*, vol. 285, Jan. 2021.

[12] M. Khoshjahan, M. Fotuhi-Firuzabad, and M. Moeini-Aghtaie *et al.*, "Enhancing electricity market flexibility by deploying ancillary services for flexible ramping product procurement," *Electric Power Systems Research*, vol. 191, Feb. 2021.

[13] X. Jin, Q. Wu, and H. Jia *et al.*, "Local flexibility markets: literature review on concepts, models and clearing methods," *Applied Energy*, vol. 261, Mar. 2020.

[14] C. A. Correa-Florez, A. Michiorri, and G. Kariniotakis *et al.*, "Optimal participation of residential aggregators in energy and local flexibility markets," *IEEE Transactions on Smart Grid*, vol. 11, no. 2, pp. 1644-1656, Mar. 2020.

[15] C. Antal, T. Cioara, and M. Antal *et al.*, "Blockchain based decentralized local energy flexibility market," *Energy Reports*, vol. 7, pp. 5269-5288, Nov. 2021.

[16] T. Morstyn, A.Teytelboym, and M. D. McCulloch *et al.*, "Designing decentralized markets for distribution system flexibility," *IEEE Transactions on Power Systems*, vol. 34, no. 3, pp. 2128-2139, May 2019.

[17] V. A. Evangelopoulos, T. P. Kontopoulos, and P. S. Georgilakis, "Heterogeneous aggregators competing in a local flexibility market for active distribution system management: a bi-level programming approach," *International Journal of Electrical Power & Energy Systems*, vol. 136, Mar. 2022.

[18] M. S. H. Nizami, M. J. Hossain, and K. Mahmud, "A nested transactive energy market model to trade demand-side flexibility of residential consumers," *IEEE Transactions on Smart Grid*, vol. 12, no. 1, pp. 479-490, Jan. 2021.

[19] W. Zhou, Y. Gao, and F. Peng *et al.*, "Peer-to-peer energy trading strategy for prosumers based on model predictive control," P*ower System Protection and Control*, vol. 50, no. 9, pp. 1-10, May 2022.

[20] X. Wang, C. Wang, and T. Xu *et al.*, "Optimal voltage regulation for distribution networks with multi-microgrids," *Applied Energy*, vol. 210, pp. 1027-1036, Jan. 2018.

[21] S. Nguyen, W. Peng, and P. Sokolowski *et al.*, "Optimizing rooftop photovoltaic distributed generation with battery storage for peer-to-peer energy trading," *Applied Energy*, vol. 228, pp. 2567-2580, Oct. 2018.

[22] J. M. Zepter, A. Lüth, and P. Crespo Del Granado *et al.*, "Prosumer integration in wholesale electricity markets: synergies of peer-to-peer trade and residential storage," *Energy and Buildings*, vol. 184, pp. 163-176, Feb. 2019.

[23] J. Dong, C. Song, and S. Liu *et al.*, "Decentralized peer-to-peer energy trading strategy in energy blockchain environment: a game-theoretic approach," *Applied Energy*, vol. 325, Aug. 2022.

[24] M. Khorasany, Y. Mishra, and G. Ledwich, "A decentralized bilateral energy trading system for peer-to-peer electricity markets," *IEEE Transactions on Industrial Electronics*, vol. 67, no. 6, pp. 4646-4657, Jun. 2020.

[25] C. Huang, M. Zhang, and C. Wang *et al.*, "An interactive two-stage retail electricity market for MGs with peer-to-peer flexibility trading," *Applied Energy*, vol. 320, Aug. 2022.

[26] L. Chen, N. Liu, and J. Wang, "Peer-to-peer energy sharing in distribution networks with multiple sharing regions," *IEEE Transactions on Industrial Informatics*, vol. 16, no. 11, pp. 6760-6771, Nov. 2020.

[27] M. J. Osborne and A. Rubinstein. "Classical models of bargaining," in *Bargaining and Markets*, San Diego, USA: Academic Press, 1990, pp. 11-39.

[28] M. He and M. Giesselmann, "Reliability-constrained self-organization and energy management towards a resilient microgrid cluster," in *2015 IEEE PES Innovative Smart Grid Technologies conference (ISGT)*, Washington, USA, pp. 1-5, Feb. 2015.

[29] E. Wei, A. Ozdaglar, and A. Jadbabaie *et al.*, "A distributed Newton method for network utility maximization-I: algorithm," *IEEE Transactions on Automatic Control*, vol. 58, no. 9, pp. 2162-2175, Sept. 2013.

[30] L. Xiao, S. Boyd, and S. Lall, "A scheme for robust distributed sensor fusion based on average consensus," in *IPSN 2005. Fourth International Symposium on Information Processing in Sensor Networks*, Boise, USA, pp. 63-70, Apr. 2005.

[31] R. Storn and K. Price, "Differential evolution—a simple and efficient heuristic for global optimization over continuous spaces," *Journal of Global Optimization*, vol. 11, no. 4, pp. 341-359, Dec. 1997.